LATERAL DYNAMICS OF NON-UNIFORM WEBS

By

Ronald P. Swanson
3M Company
USA

ABSTRACT

A new method of generating and testing cambered web has been developed. Experimental lateral static data is presented for twenty six different conditions and dynamic data is presented for five of these conditions. Numerous models have been proposed to describe the static and dynamic lateral behavior of non-uniform webs. Despite the plethora of theoretical hypotheses, debate continues about the direction, not to mention the magnitude, of lateral displacement of a cambered web. Previously presented models and data are discussed in light of these new experimental findings.

NOMENCLATURE

L	Span length
T	Tension
t	Web thickness
W	Web width
y	Lateral deflection
y'	Slope, dy/dx
y''	Curvature, d^2y/dx^2
κ	Curvature
ρ	Radius of curvature

Subscripts:

0	X=0, upstream end of the beam
L	X=L, Downstream end of the beam
web	Referring to non-tensioned web

GENERATION OF NON-UNIFORM WEB

Advances in motor/drive technology have enabled accurate coordination of multi-axis systems. This technology was used to make a laterally shifting slitting system with the capability of cutting an accurate, large radius (cambered) web, from an initially wider longitudinally advancing web. The cambered sections of web were separated by straight sections that were used as reference for the lateral position sensors.

Laterally Shifting Slitting System

Figure 1 illustrates a linear actuator mounted adjacent to a web span. The slitter blades, shown in Figure 2, are both rigidly attached to the slitter frame. The frame was laterally positioned by the linear actuator.

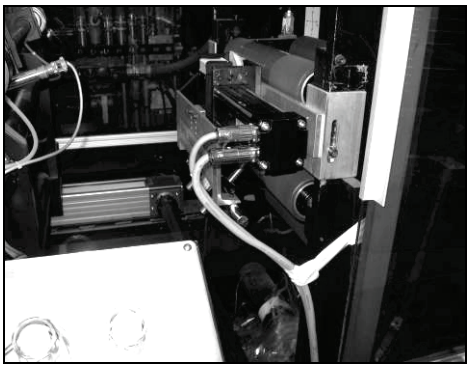

Figure 1 – Linear Actuator

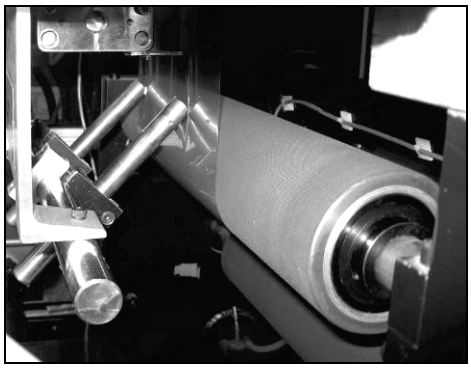

Figure 2 – Laterally Shifting Slitter

Experimental Setup

The laterally shifting slitter was placed on the unwind stand of an experimental web line, as shown in Figure 3. The unwind stand was configured to provide sidelay web guiding. The web guiding system provided for a uniform lateral position at the sidelay sensor. The web then traveled over a pull roller, which was the line speed pacer. After the pull roller the web was guided a second time with an Offset Pivot Guide (OPG). Next the web was guided a third time, just upstream of the test span. These guides provided for the first boundary condition of $y_0 = 0$, as can be seen by the very small values in the y_L column of Table 2. The tension was controlled by the pull roller and loadcell downstream of the test stand. An additional load cell was used upstream of the test stand to monitor test section web tension. Figure 4 is a scaled CAD drawing of the test stand web path.

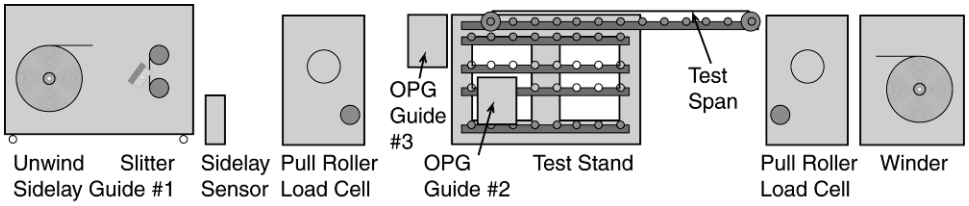

Figure 3 – Experimental Webline Layout

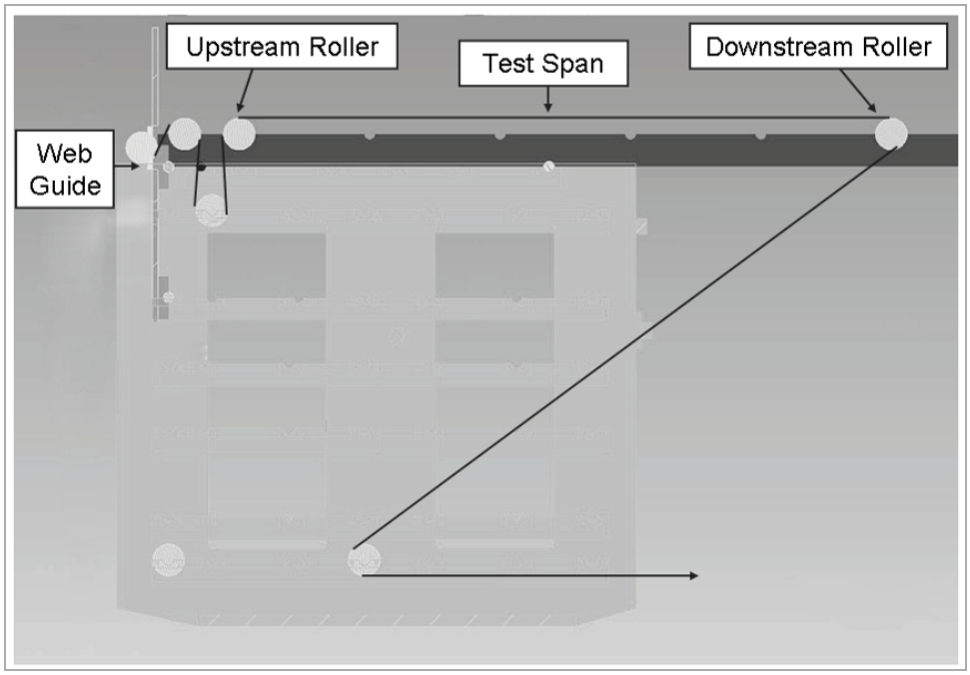

Figure 4 – Scaled Drawing of the Test Section Web Path

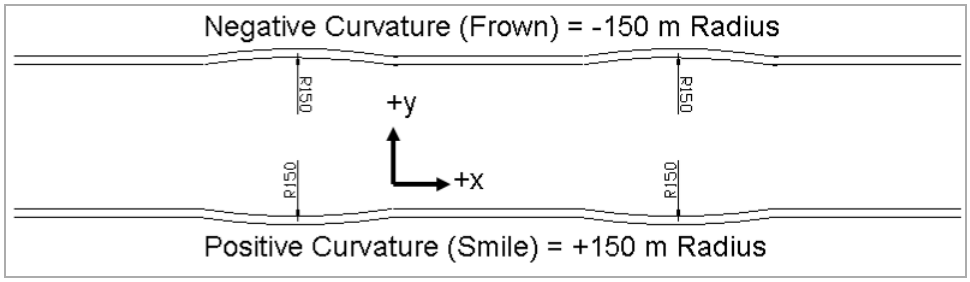

Figure 5 – Coordinate System and Sign Convention

A coordinate system and sign convention was established as shown in Figure 5. Figure 6 shows a section of experimental web that was used to confirm web shape with cord and cord height measurements.

Some slackness could be seen in the web span as the abrupt change in slope, at the beginning and end of the sample, passed through the test section along with large lateral excursions. All experimental runs were designed with at least 6 L/V (length/velocity) time constants between changes to insure steady state operation could be observed. Figure 7 is a low angle view, from the downstream end test span, as seen during steady state passing of a cambered web section. This picture illustrates that the span is free of slackness and wrinkling.

Figure 6 – Cambered Web Sample

Figure 7 – Wrinkle Free Web

Experiment

Table 1 lists experimental constants. Experimental variables included the radius cut into the web (ρ_{web}), test span length (L), web tension (T), upstream traction and downstream traction. Cord length was selected to give the longest length cambered section that could be cut out of the original 300 mm (12 in.) width web. Straight sections were set to equal the cambered sections. No attempt was made to smooth the transition between the straight and cambered sections. This resulted in discontinuity and severe lateral motion as it passed through the test span.

Web Material	PET			
Thickness	50	μm	0.002	in.
Width	0.1524	m	6	in.
Modulus	4482	Mpa	650000	psi
Speed	0.127	m/s	25	fpm
Roller Diameter	75	mm	2.95	in.

Table 1 – Experimental Constants

Dynamic lateral position data was taken for the entry and exit points of the test spans. Plots of the dynamic response for select conditions are presented in the "*Results*" section of this report. Static lateral position data was taken as the average value of the dynamic data measured in the steady state region of operation. Static lateral position data is presented in Table 2.

Experimental Results

Figure 8 is a graph of the lateral dynamics of alternating straight and curved web sections passing through the test span. The lateral position of the web is perturbed at the output, and to a lesser degree the input, as the transition passes through the test span. It can be seen that steady state has been attained before the arrival of the next transition. Figure 9 is a blown up view of Figure 8, and clearly shows that under these conditions there is no steady state lateral deflection of the curved section of the web.

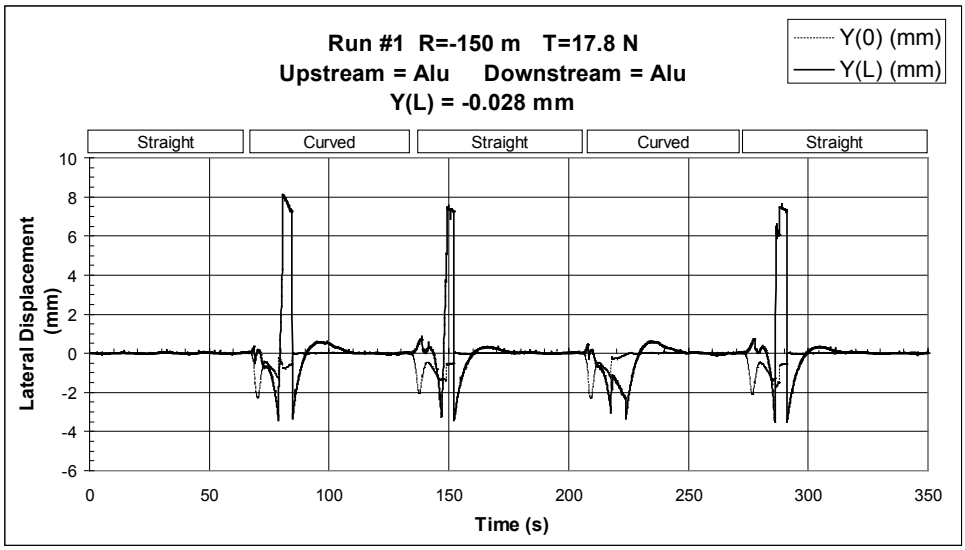

Figure 8

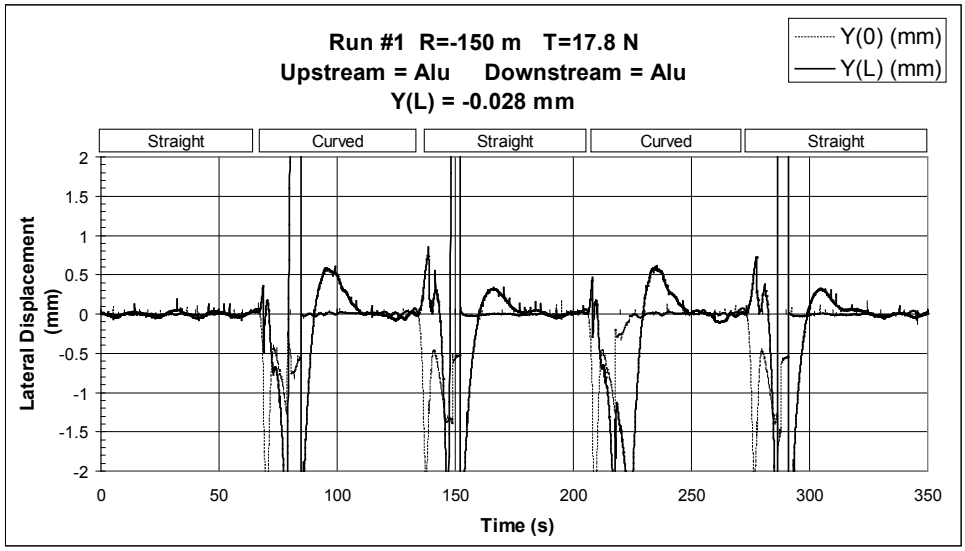

Figure 9

Figure 10 and Figure 11 conditions show similar to the previous figures, with the exception of higher friction surfaces being added to the upstream and downstream rollers. A steady state offset can clearly be seen at the end of the test span.

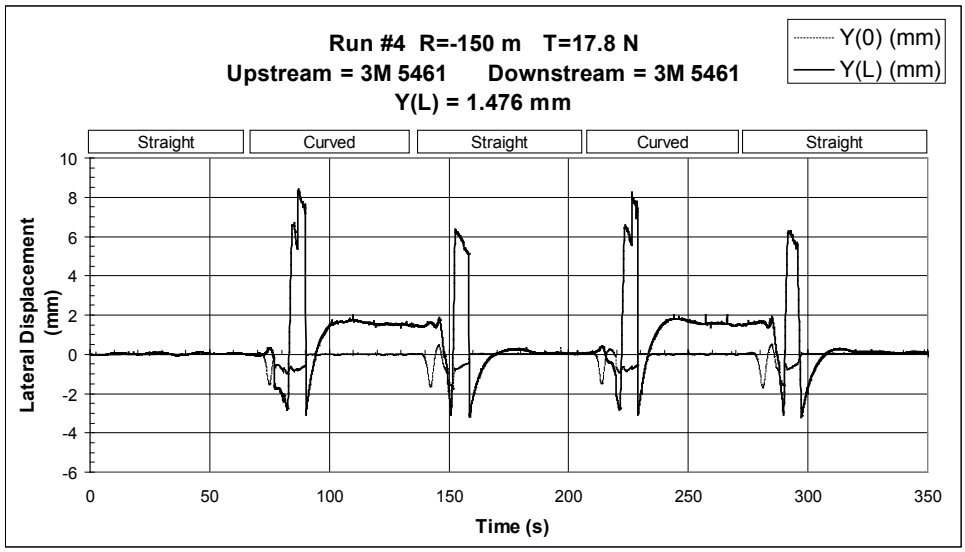

Figure 10

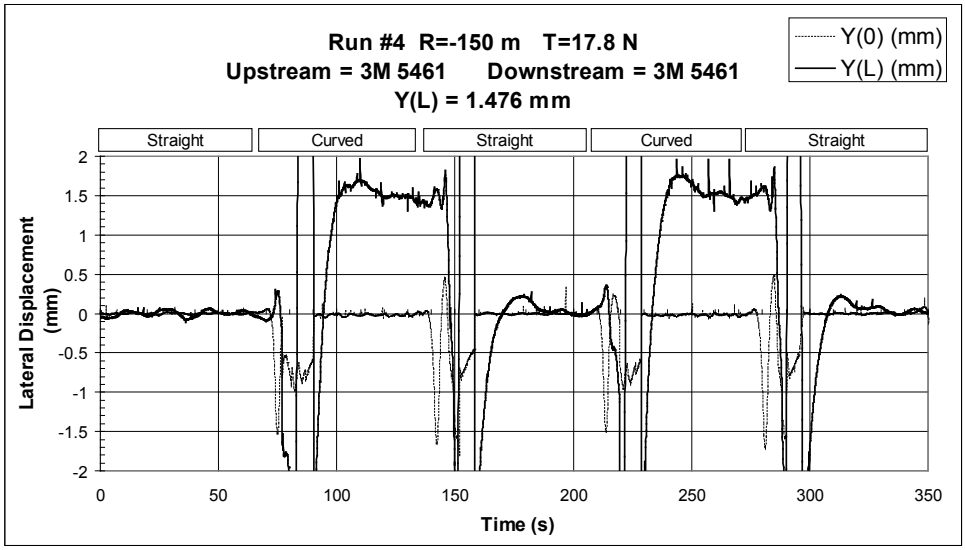

Figure 11

Figure 12 and Figure 13 are similar to the previous figures, except for the direction of the curvature. Comparison with Figure 10 and Figure 11 illustrates that the test method is symmetric.

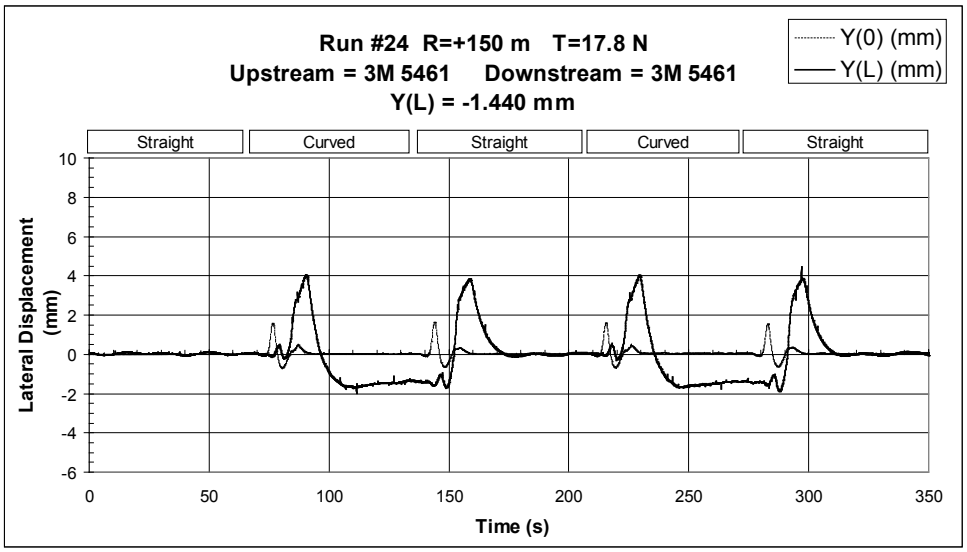

Figure 12

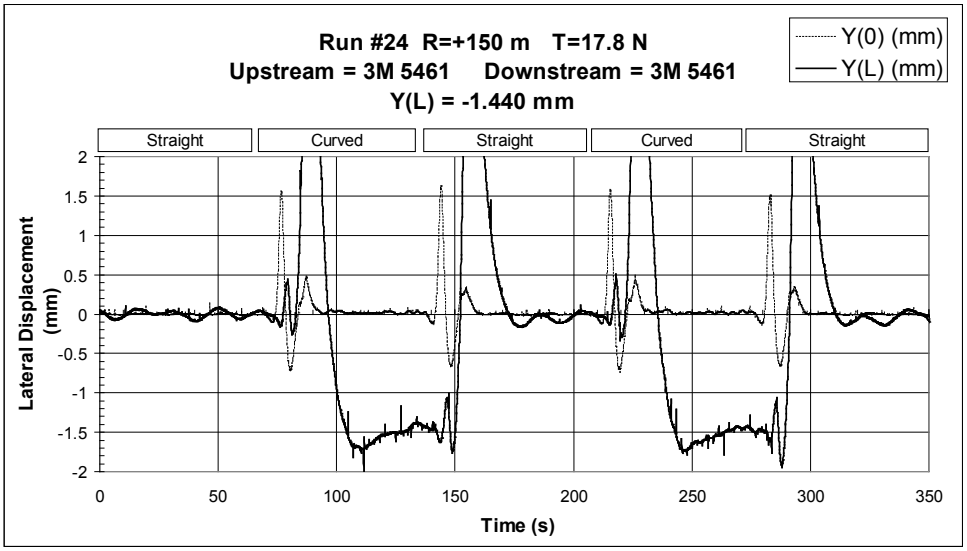

Figure 13

Figure 14 and Figure 15 show the response when just the downstream roller is covered in high traction tape. The cambered web clearly has a steady state lateral deflection.

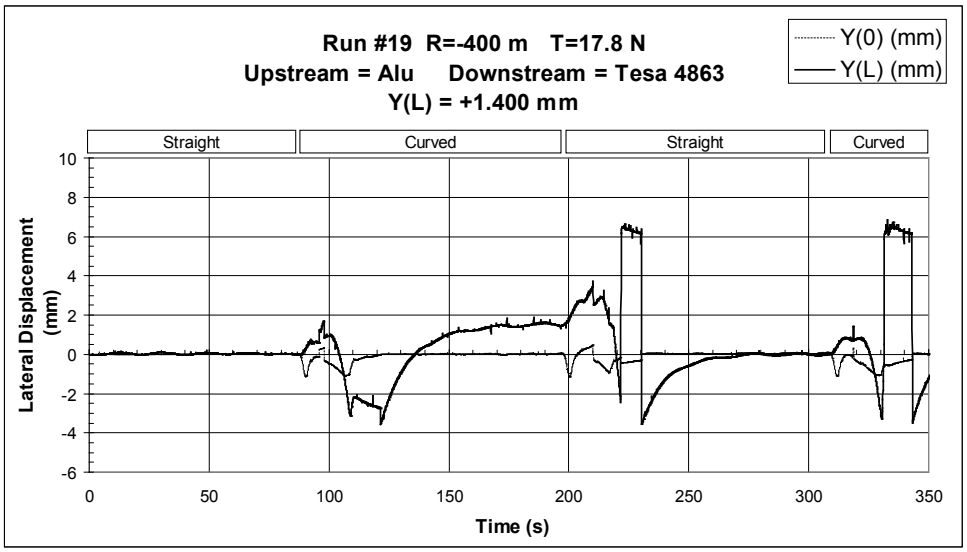

Figure 14

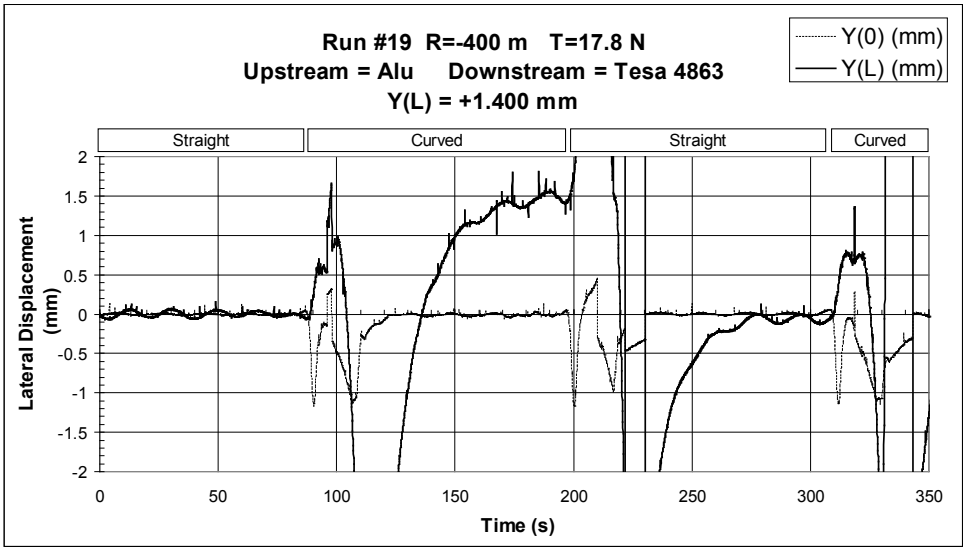

Figure 15

Figure 16 and Figure 17 show that there is no steady state lateral deflection in the cambered web when just the upstream roller is wrapped with high traction tape. This is in contrast to Figure 14 and Figure 15, which both exhibit deflection when just the downstream roller is covered.

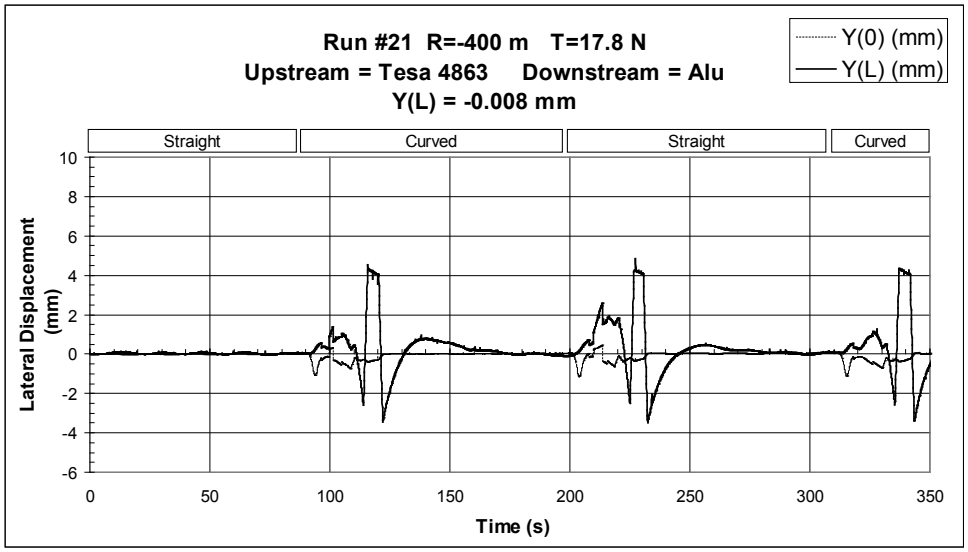

Figure 16

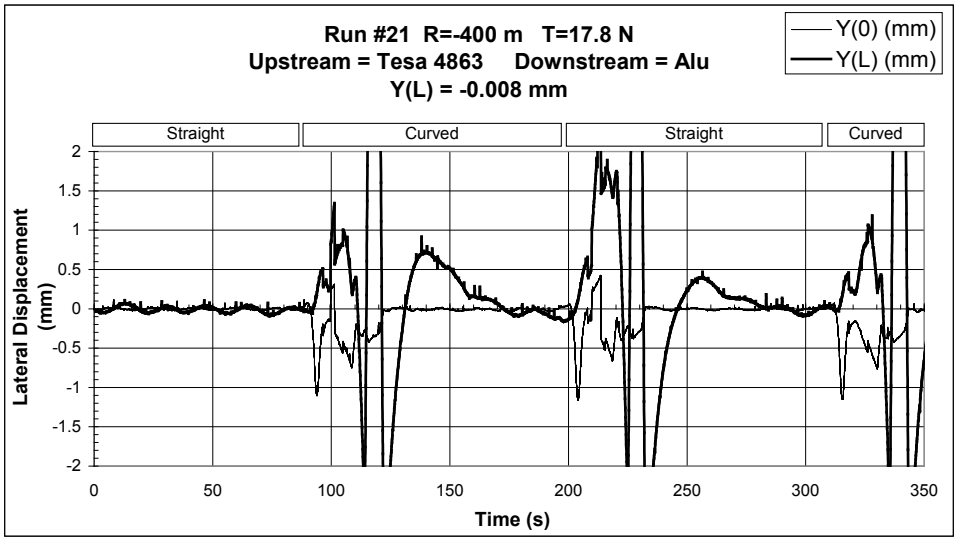

Figure 17

A summary of conditions and steady state responses is given in Table 2

Run	Camber Direction	ρ_{Web} (m)	Cord (m)	Span (m)	Tension (N)	Traction Upstream	Traction Downstream	Critical Tension (N)	Critical Tension (%)	y(0) (mm)	y(L) (mm)	ρ_L [4] Eq. (25) (m)	ρ_{Web}/ρ_L
1	-1	150	9	1.52	17.8	Alum. (0.8 μm)	Alum. (0.8 μm)	17.6	101	0.010	-0.028	13712	0.01
2	-1	150	9	1.52	35.6	Alum. (0.8 μm)	Alum. (0.8 μm)	17.6	202	0.010	0.061	6222	0.02
3	-1	150	9	1.52	53.4	Alum. (0.8 μm)	Alum. (0.8 μm)	17.6	303	0.013	0.028	13440	0.01
4	-1	150	9	1.52	17.8	3M 5461 Tape	3M 5461 Tape	17.6	101	-0.010	1.476	260	0.58
5	-1	150	9	1.52	35.6	3M 5461 Tape	3M 5461 Tape	17.6	202	0.000	0.302	1255	0.12
6	-1	150	9	1.52	53.4	3M 5461 Tape	3M 5461 Tape	17.6	303	-0.003	0.064	5914	0.03
7	-1	150	9	1.52	17.8	Tesa 4863	Tesa 4863	17.6	101	0.015	1.295	296	0.51
8	-1	150	9	1.52	35.6	Tesa 4863	Tesa 4863	17.6	202	0.015	0.919	412	0.36
9	-1	150	9	1.52	53.4	Tesa 4863	Tesa 4863	17.6	303	0.020	0.630	596	0.25
10	-1	300	12	1.52	17.8	Alum. (0.8 μm)	Alum. (0.8 μm)	8.8	202	0.010	0.013	30167	0.01
11	-1	300	12	1.52	35.6	Alum. (0.8 μm)	Alum. (0.8 μm)	8.8	404	0.008	0.030	12443	0.02
12	-1	300	12	3.05	35.6	Alum. (0.8 μm)	Alum. (0.8 μm)	8.8	404	0.005	0.163	8815	0.03
13	-1	300	12	1.52	17.8	3M 5461 Tape	3M 5461 Tape	8.8	202	-0.015	0.813	471	0.64
14	-1	300	12	1.52	35.6	3M 5461 Tape	3M 5461 Tape	8.8	404	0.000	0.114	3318	0.09
15	-1	400	14	3.05	17.8	Alum. (0.8 μm)	Alum. (0.8 μm)	6.6	269	-0.008	0.015	97604	0.00
16	-1	400	14	3.05	35.6	Alum. (0.8 μm)	Alum. (0.8 μm)	6.6	539	0.008	0.023	62686	0.01
17	-1	400	14	3.05	17.8	Tesa 4863	Tesa 4863	6.6	269	-0.005	1.364	1091	0.37
18	-1	400	14	3.05	35.6	Tesa 4863	Tesa 4863	6.6	539	-0.005	1.242	1154	0.35
19	-1	400	14	3.05	17.8	Alum. (0.8 μm)	Tesa 4863	6.6	269	-0.008	1.400	1063	0.38
20	-1	400	14	3.05	35.6	Alum. (0.8 μm)	Tesa 4863	6.6	539	0.003	1.052	1363	0.29
21	-1	400	14	3.05	17.8	Tesa 4863	Alum. (0.8 μm)	6.6	269	-0.005	-0.008	195207	0.00
22	-1	400	14	3.05	35.6	Tesa 4863	Alum. (0.8 μm)	6.6	539	-0.018	0.109	13120	0.03
23	1	150	9	1.52	35.6	Alum. (0.8 μm)	Alum. (0.8 μm)	17.6	202	0.013	0.058	6492	0.02
24	1	150	9	1.52	17.8	3M 5461 Tape	3M 5461 Tape	17.6	101	0.013	-1.440	266	0.56
25	1	150	9	1.52	35.6	3M 5461 Tape	3M 5461 Tape	17.6	202	0.003	-0.302	1255	0.12
26	1	150	9	1.52	53.4	3M 5461 Tape	3M 5461 Tape	17.6	303	0.005	-0.0762	4928	0.03

Table 2 – Experimental Results[1]

MAIN EFFECTS

Figure 18 is a graphical representative of how the chosen levels of input affect the deflection at the downstream roller. Caution should be taken while interpreting the results of this Main Effects Plot, as the experimental input data was not a symmetric factorial design.

[1] Data analysis performed by Dr. J. K. Good

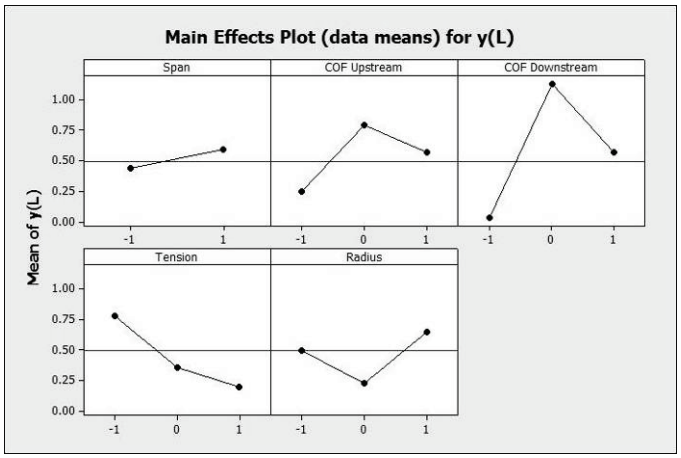

Figure 18 – Main Effects Plot

PARETO PLOT

Figure 19 is a plot of how the input variables affect the ratio ρ_{web}/ρ_L. Caution should be taken while interpreting the results of this Pareto Plot, as the experimental input data was not a symmetric factorial design. This plot is similar to Figure 7 of Swanson [4], but illustrates a very different conclusion. The new data suggests that the friction of the down stream roller is the only significant predictor of the ratio ρ_{web}/ρ_L. The previous data suggested that friction was not significant, but span length was significant.

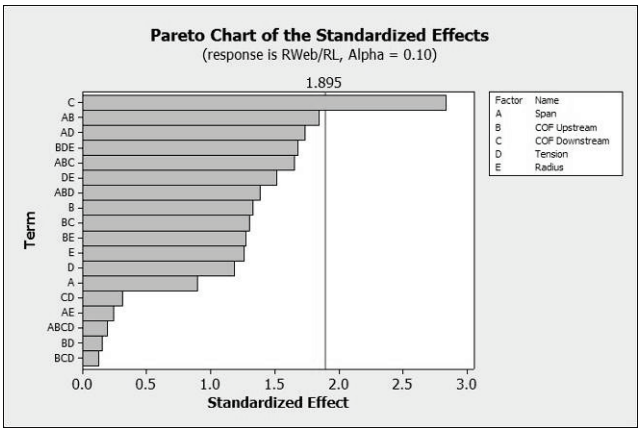

Figure 19 –23 Pareto Plot of ρ_{web}/ρ_L

ON THE APPLICABILITY OF B.C. #2 ($Y'_0 = 0$)

The small values in the Y_0 column of Table 2 , constitute proof of the validity of the experimental test setup, the web guide and the applicability of the commonly used B.C. #1 ($y_0 = 0$). Figure 20 and Figure 21 Figure 21are pictures taken of the upstream roller during the steady-state phase of the positive and negatively cambered web. These pictures suggest that the slope at the upstream roller may not be zero. The rollers in these

figures are wrapped with 3M 5461 Tape. This tape has a very smooth silicone rubber surface, providing a COF well above one, but almost no peel force (adhesion).

Figure 20 shows a lack of surface wetting on the foreground end of the upstream roller. When this picture was taken, the foreground side of the web was the low tension or "baggy" side. The lack of wetting suggests that there may be some "*induced taper*" effect at low tension levels as suggested by Shelton [3].

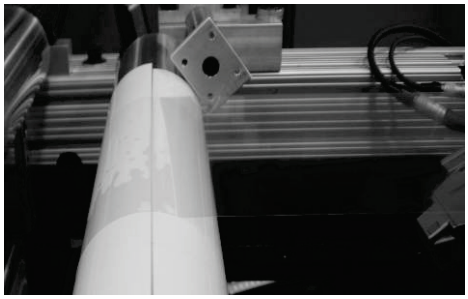

Figure 20

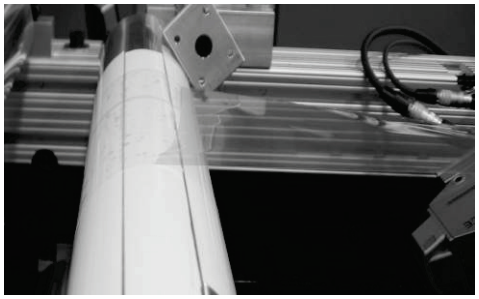

Figure 21

SUMMARY OF PREVIOUS PAPERS ON NON-UNIFOM WEB MECHANICS

Shelton [1]

"*Lateral Dynamics of a Moving Web*" [1] was the original effort in web mechanics. The web statics section established four boundary conditions.

BC#1, the first upstream boundary condition was $y_0=0$.

$$y \text{ is chosen to be zero at } x = 0,$$

BC#2, the second upstream boundary condition was $y'_0=0$

$$\text{at } x = 0, \frac{dy}{dx} = 0.$$

BC#3, the first downstream boundary condition was $y'_L= \theta$

That a web approaches a roller perpendicularly to the roller axis

BC#4, The second downstream boundary condition was that no moment can exist at the downstream end of the web.

$$M_L = 0$$

These boundary conditions were used to solve a fourth order differential equation, resulting in equations that model static deflection, moment and shear. Shear and deflection measurements were used to verify the model.

This work was not focused on cambered web, but does state that "*because of web imperfections and inexact methods of observation, it might be questioned if the moment*

has entirely disappeared at the guide roller. But the test of Figure 2.2.7 has been presented as proof that M_L is equal to zero."

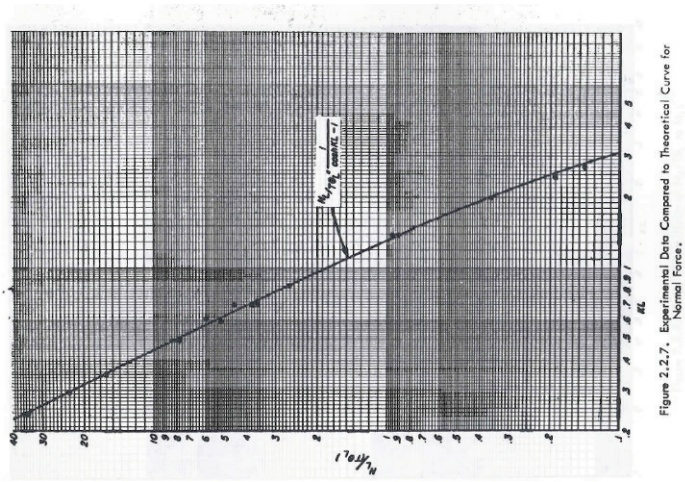

Figure 2.2.7. Experimental Data Compared to Theoretical Curve for Normal Force.

Shelton also considered the consequences of a non-zero M_L: "*The fourth necessary boundary condition, that the moment on the guide roller is zero in steady state, is not immediately obvious. Its experimental determination, representing one of the primary contributions of this thesis, is reported in Section 2.2. However, it seems appropriate to digress at this point to give an intuitive proof of this crucial boundary condition.*

Imagine that an initially straight and uniform web in its steady state position has a residual negative moment as it makes contact with a roller. The web has a finite radius of curvature, as shown in Figure 2.1.3, which means that the web is longer on one side than the other. If the roller were composed of many short, independent rollers instead of a single body, the roller at the left side of the web would turn fastest, because more length of web is passing over it per unit time. Similarly, the roller on the right end would turn slowest. But both ends of the single roller must turn at the same speed. Thus, because the left side of the web in Figure 2.1.3 would be trying to turn the roller faster and the right side slower, the roller would exert a positive moment on the web until the negative moment was cancelled as a result of the web movement, if the friction forces were sufficient. The initial assumption of a steady-state moment was incorrect, so the steady-state moment at the downstream end of the free span must be zero."

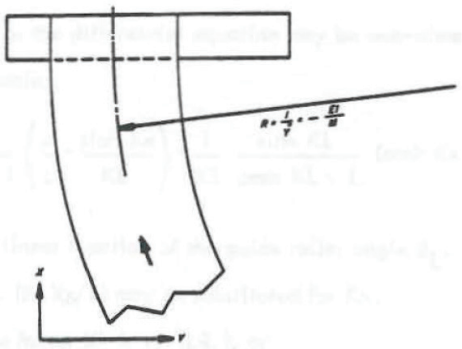

Figure 2.1.3. Web With Moment at Guide Roller.

Swanson [2]

"*Air Support Conveyance of Uniform and Non-Uniform Webs*" [2] described the mechanics of cambered webs. Three solution techniques were presented including a numerical model, a finite element model and a closed form equation. The boundary conditions were established as follows

BC#1, the first upstream boundary condition was $y_0=0$.

$$y(0) = 0.$$

BC#2, the second upstream boundary condition was $y'_0=0$

$$y'(0) = 0$$

BC#3, the first downstream boundary condition was $y'_L=0$, Tram error was not considered.

$$y'(L) = 0$$

BC#4, the second downstream boundary condition was that no curvature can exist at the downstream end of the web. The exception to this would be in situations of long L/W ratios or when traction was insufficient to remove downstream curvature. In these cases the curvature at the downstream roller would assume the natural curvature of the untensioned web.

L/W <10, High Traction $y''(L) = 0$

L/W >10, Low Traction $y''(L) = -\frac{M_0}{EI}$

The web shape deflection data was presented for two cases, first showing a short web span with only slight deflection at midspan and no deflection at the end of the span. The second, much longer span shows the web tracking to the long side of the cambered web.

Shelton [3]

"*Effects of Cambered Web on Handling*" [3] discussed web camber and the problems associated with the handling of cambered webs, and several useful equations were presented. The equation for critical tension, the minimum tension required to eliminate slackness in all parts of the web, was presented as $T_{cr}=EtW^2/2\rho$.

Limited data was presented from tests of cambered belts run in the 1969-1971 and 1997 timeframe. The cambered belt was run over rollers and the tram error needed to stabilize the lateral motion was measured.

A mechanism, called induced taper, was introduced to explain why webs have been observed to deflect toward the baggy side. The low-tension side of the web would ride higher on the roller and therefore behave as a tapered roller.

Swanson [4]

"Mechanics of Non-Uniform Webs," [4] presented the results of a factorially designed experiment to investigate lateral deflection of non-uniform webs between two parallel rollers. This was the first publication of lateral deflection data with varying input settings and has been subsequently used to test numerous theoretical models.

First, closed form equations were developed based on an arbitrary constant moment, producing a curvature of $-1/\rho$ at x=L.

BC#1, the first upstream boundary condition was $y_0=0$.

$$y(0) = 0.$$

BC#2, the second upstream boundary condition was $y'_0=0$

$$y'(0) = 0$$

BC#3, the first downstream boundary condition was $y'_L=\theta$

$$y'_L = \theta$$

BC#4, the second downstream boundary condition was that the curvature set equal to an arbitrary constant of $-1/\rho$ at x=L.

$$M_1 = \text{Constant} \therefore y''_L = -\frac{C}{EI} = -\frac{1}{\rho_L}$$

The non-uniform web was produced by winding shim material into a roll of PET film and baking the roll above the T_g of the film to produce permanently longer web in the shimmed area. A unique unwind was built that could measure the small shear forces in the web span. Experimental data was fit to the resulting closed form equations to determine the actual curvature at the end of the beam.

Span (m)	COF	Tcr (N)	T(N)	Y_L (mm)	ρ_L (m)	ρ_{web} (m)	ρ_L/ρ_w
0.67	0.20	22	22	-0.12	534	185	0.35
2.00	0.20	22	66	-0.30	1842	139	0.08
0.67	1.00	22	66	-0.16	388	115	0.30
2.00	1.00	22	22	-0.24	2319	232	0.10
0.67	0.20	66	66	-0.25	254	85	0.33
2.00	0.20	66	22	-0.75	*751	68	*0.09
0.67	1.00	66	22	-0.18	351	68	0.19
2.00	1.00	66	66	-0.29	1885	65	0.03
1.33	0.30	44	44	-0.08	3094	111	0.04
* Denotes Web Tension < Tcr (term corrected for tensioned web width)							

The following conclusions were made:

1. Cambered webs do induce shear and deflection in trammed web spans. The web will deflect toward the baggy side and have shear forces consistent with the amount of deflection. The shear and deflection values are quite small in relation to factors such as tram error.
2. The actual fourth boundary condition is not $Y''_0=0$ or $Y''_0=1/\rho_{web}$, but is bracketed by these values. This boundary condition does not seem to be a function of tension or friction, but is related to span length.
3. The effect of cambered web on lateral deflection, shear and moment is to add an offset the values predicted by Shelton[1]
4. Shear deflection and possibly moment measurements can be used to quantify the effects of cambered web.
5. Shelton's tapered roller theory is probably not an explanation of cambered web behavior.

The conclusion statement "*This boundary condition does not seem to be a function of tension or friction*" was based on a Pareto analysis of the ratio of the radius of curvature at the downstream roller (ρ_L) and the radius of curvature of the untensioned web (ρ_{web}). This analysis indicated that tension or friction were not good predictors of this ratio.

Benson [5]

"*The Influence of Web Warpage on Lateral Dynamics of Webs*", [5] presents a lateral dynamics model of a sinusoidally warped web modeled with linear elastic beam theory that allows the web to have a non-flat, stress free state. The model predicts that even if the sinusoidally warped web enters a span without deflection or slope, lateral motion will be induced at the downstream roller. Additionally, if the downstream roller was displaced or rotated to eliminate lateral deflection at that point, midspan lateral deflection would persist.

Sinusoidally warped web was added into the moment/curvature relationship through the ϕ^* term as shown below.

$$\textit{Moment / curvature relationship:} \quad \frac{d\psi}{dx} = \frac{d\phi^*}{dx} + \frac{M}{EI}$$

BC#1, the first upstream boundary condition was the lateral dynamics version of $y_0=0$

$$w_o = \text{known function of time.}$$

BC#2, the second upstream boundary condition was the lateral dynamics version of $y'_0=0$

$$\psi_o = \text{known function of time.}$$

BC#3, the first downstream boundary condition was that the time derivative of the lateral position was equal to the sum of the lateral velocity of the web walking on the roller due to the roller angle, the lateral velocity of the web due to it's sinusoidal warp and the lateral velocity of the roller.

$$\frac{dw_L}{dt} = v(\theta - \phi_L) + \frac{dZ}{dt}$$

BC#4, the second downstream boundary condition was that no moment can exist at the downstream end of the web.

$$M_L = 0 .$$

Several numerical examples were given, but no experimental verification was presented.

Roisum [6]

"*Web Bagginess: Making, Measurement and Mitigation Thereof*" [6], is a general overview of web bagginess. It defines web bagginess based on variations of flatness, stress and strain. The paper goes on to discuss web handling problems associated with web bagginess, measurement techniques and sources of web bag.

Olsen [7, 8]

"*Lateral Mechanics of an Imperfect Web*" [7, 8], presents a model based on elementary beam theory and parallels the work of Shelton [1]. Frozen in strain is not accounted for by elementary beam theory or Shelton [1] and was added into the constitutive equation as ε_i. The boundary conditions were the same as Shelton [1].

$$\sigma(y) = E(y)\varepsilon_0 - E(y)\varepsilon_i(y) + E(y)\kappa y$$

BC#1, the first upstream boundary condition was $y_0=0$.

$$u = 0 \qquad u' = 0 \qquad \text{at } x = 0$$

BC#2, the second upstream boundary condition was $y'_0=0$

$$u = 0 \qquad u' = 0 \qquad \text{at } x = 0$$

BC#3, the first downstream boundary condition was $y'_L=\theta$

$$u' = \theta_L \qquad \text{at } x = L$$

BC#4, the second downstream boundary condition was that no moment can exist at the downstream end of the web.

$$M = 0 \text{ at } x = L,$$

This formulation resulted in nonzero ρ_L, as experimentally found by Swanson [4], while still using the M_L=0 fourth boundary condition. The shape and direction of the deflection was consistent with Swanson [4].

Benson [9]

"*Lateral Dynamics of a Moving Web with Geometrical Imperfection*" [9] improves "*The Influence of Web Warpage on Lateral Dynamics of Webs*" [5] model by accounting for the contributions of roller tilt. The boundary conditions are based on the assumptions "*It is assumed that the web sticks to the downstream roller at all points of first contact:*" and "*It is further expected that the web will stick to the roller for all points of first contact-not just at the web's centerline. To achieve that, we must also match the rotational velocities of the roller and web face*".

BC#1, the first upstream boundary condition was the lateral dynamics version of y_0= 0

$$w(0) = w_0$$

BC#2, the second upstream boundary condition was the lateral dynamics version of y'_0=θ

$$\frac{dw_L}{dt} = v(\theta - \phi_L) + \frac{dZ}{dt}.$$

BC#3, the first downstream boundary condition was that the time derivative of the lateral position was equal to the sum of the lateral velocity of the web walking on the roller due to the roller angle, the lateral velocity of the web due to it's sinusoidal warp and the lateral velocity of the roller.

$$\frac{d\theta}{dt} = \left.\frac{d\psi}{dt}\right|_L = \left(\frac{\partial\psi}{\partial t} + \frac{\partial\psi}{\partial x}\frac{\partial x}{\partial t}\right)_L = \left(\frac{\partial\psi}{\partial t} + \frac{\partial\psi}{\partial x}v\right)_L$$

BC#4, the second downstream boundary condition was that no moment can exist at the downstream end of the web. Benson [9] states "These boundary conditions fall within the acceptable set produced by virtual work analysis".

$$\frac{d\psi_L}{dt} = \frac{d\theta}{dt} - v\left[\frac{M_L}{EI} + \frac{d\phi_L^*}{dx}\right]$$

This paper presents a model that would result in no steady state offset at the downstream end of a span transversed by a uniformly cambered web. The models prediction, contrary to the experimental results presented in Swanson [2, 4] were explained "*It is the author's belief that the baggy side deflection in the Swanson study was likely caused by the partial buckling or wrinkling of the web*".

Olsen [10]

"*Shear Effects and Lateral Dynamics of Imperfect Webs*" [10], presents an extension of the "*Lateral Mechanics of an Imperfect Web*" [7, 8] papers which include shear and web dynamics.

BC#1, the first upstream boundary condition was $y_0=0$.

$$u = 0 \qquad \text{at } x = 0$$

BC#2, the second upstream boundary condition includes shear effects.

$$\frac{\partial u}{\partial x} = \gamma_o \qquad \text{at } x = 0$$

BC#3, the first downstream boundary condition was $y'_L=\theta$

$$u' = \theta_L \qquad \text{at } x = L$$

BC#4, the second downstream boundary condition.

$$\left.\frac{\partial^2 u}{\partial x^2}\right|_{x=L} = \frac{1}{V_x^2}\frac{d^2 u_L}{dt^2} - \kappa_L - \frac{1}{V_x^2}\frac{d^2 z}{dt^2} - \frac{1}{V_x}\frac{d\gamma_L}{dt}$$

This formulation resulted in nonzero ρ_L, as experimentally found by Swanson [4], while still using the fourth boundary condition. The shape and direction of the deflection was consistent with Swanson [4].

Olsen [11]

"*Lateral Mechanics of Baggy Webs at Low Tensions*" [11] extends the "*frozen in strain*" theory developed in [7, 8, and 10] to a dynamics model that includes sections of the span that do not support compressive stresses. The model uses an iterative non-linear finite difference method solution.

BC#1, **BC#2, BC#3** are the same as [10].

BC#4, the second downstream boundary condition:

$$u'' = -\kappa_{web} \qquad \text{at } x = L$$

The model results show "*the lateral deflection of perfect webs and baggy webs is significantly affected by tension at the lower levels of tension*". Numerical examples are given for PET Web comparable to Swanson [4].

Brown [12]

"*Effects of Concave Rollers, Curved-Axis Rollers and Web Camber on the Deformation and Translation of a Moving Web*" [12] uses two-dimensional plane stress and nonlinear theory of elastic in a finite element method solution.

BC#1, the first upstream boundary condition was $y_0=0$.

$$u = 0.$$

BC#2, the second upstream boundary condition includes shear effects.

$$\text{uniform, } \varepsilon_x' \quad v = -\mu \int \varepsilon_x dy + C$$

BC#3, the first downstream boundary condition was $y'_L=\theta$

BC#4, the second downstream boundary condition was the normal strain condition.

$$\varepsilon_x = 1 - \frac{V_u}{V_d}\frac{R_o - y}{R_o}(1 - \varepsilon_{xo})$$

The results of this model were compared with the experimental results of Swanson [4] and found to be in the same direction, but lower in magnitude.

Jones [13]

"*Web Sag and the Effects of Camber on Steering*" [13] is an ABAQUS finite element model that includes the effect of gravity and sag.

BC#1, the first upstream boundary condition was $y_0=0$.

At the upstream roller, the lateral position y of the web is fixed.

BC#2, the second upstream boundary condition was $y'_0=0$

zero angle as the web leaves the upstream roller.

BC#3, the first downstream boundary condition was $y'_L=\theta$

the normal entry rule sets the angle of entry,

BC#4, the second downstream boundary condition was the normal strain condition.

fourth boundary condition is zero web curvature at the end of the span.

The results of this model predicts that "*a cambered web steers towards the high tension side when sag is present and traction is good*" and "*The steering effect is large at low tensions*".

CONCLUSIONS

Cambered webs that travel between parallel high traction rollers, while remaining taught and free of wrinkles and troughs deflect slightly toward the low tension side of the web.

Cambered webs that travel between parallel low traction rollers, while remaining taught and free of wrinkles and troughs do not deflect laterally.

The curvature condition at the downstream end of the span is bounded between zero and the natural curvature of the untensioned cambered web ($0 \le \kappa_L \le \kappa_{web}$). This curvature will approach zero under conditions of low traction, high tension and short

spans. The curvature will approach the natural curvature of the untensioned cambered web under conditions of high traction, low tension and long spans.

Web-roller traction is very important, especially at the downstream roller.

Qualitative evidence suggests that a cambered web may not enter a span perpendicular to the upstream roller.

RECOMENDATIONS

This paper presents the first experimental lateral dynamics data for cambered web. It also presents high quality lateral statics data for a wide variety of conditions. This data could be used to check the validity of present and future models.

There has been much debate about the forth boundary condition needed to model non-uniform. Qualitative data presented in this paper suggests that the second boundary condition ($y'_0=0$) may also need more study.

Unlike previous data, this result suggests that traction is very important. A simple single span model that neglects friction may not be capable of accurate prediction. A multi-span model, which includes the effects of friction may be required for accurate prediction of the effects of non-uniform web.

ACKNOWLEDGMENTS

I would like to thank Dan Carlson for preparing the slitter actuator, drive, programming and expertise needed to implement the laterally shifting slitter. I would also like to thank Jonathan O'Hare for web path CAD, planning and assembly. I would like to thank 3M for providing the equipment and time necessary to continue this effort in fundamental understanding of web mechanics and for the permission to present this paper.

Last but not least, I would like to thank Dr. J. K. Good for his experimental and data analysis efforts, and particularly for his suggestion to use high traction tape. His suggestion was critical ensuring that the experimentation didn't ended early, with a misleading result.

REFERENCES

1. Shelton, J. J., "Lateral Dynamics of a Moving Web," Ph.D. Thesis, Oklahoma State University, Stillwater, Oklahoma, July 1968.
2. Swanson, R. P., "Air Support Conveyance of Uniform and Non-Uniform Webs," Proceedings of the 2nd International Conference on Web Handling, ed. Good, J. K., 1993, pp. 1-20
3. Shelton, J. J., "Effects of Web Camber on Handling," Proceedings of the 4th International Conference on Web Handling, ed. Good, J. K., 1997, pp. 248·264.
4. Swanson, R. P., "Mechanics of Non-Uniform Webs," Proceedings of the 5th International Conference on Web Handling, ed. Good, J. K., 1999, pp. 443-459.
5. Benson, R.C., "The Influence of Web Warpage on Lateral Dynamics of Webs," Proceedings of the 5th International Conference on Web Handling, ed. Good, J. K., 1999, pp. 461-472.
6. Roisum, D. R., "Web Bagginess: Making, Measurement and Mitigation Thereof," Proceedings of the 6th International Conference on Web Handling, ed. Good, J. K.., 2001, pp. 355-370.
7. Olsen, J. E., "Lateral Mechanics of an Imperfect Web," Proceedings of the 6th International Conference on Web Handling, ed. Good, J. K., 2001, pp. 457-468.

8. Olsen, J. E., "Lateral Mechanics of an Imperfect Web," Journal of Pulp and Paper Science, 2002, pp. 310-314.
9. Benson, R.C., "Lateral Dynamics of a Moving Web with Geometrical Imperfection," Journal of Dynamic Systems, Measurement, and Control, Vol. 124, March 2002, pp. 25-34.
10. Olsen, J. E., "Shear Effects and Lateral Dynamics of Imperfect Webs," Proceedings of the 7th International Conference on Web Handling, ed. Good, J. K., 2003.
11. Olsen, J. E., "Lateral Mechanics of Baggy Webs at Low Tensions," Proceedings of the 8th International Conference on Web Handling, ed. Good, J. K., 2005, pp. 25-37.
12. Brown, J. L., "Effects of Concave Rollers, Curved-Axis Rollers and Web Camber on the Deformation and Translation of a Moving Web," Proceedings of the 8th International Conference on Web Handling, ed. Good, J. K., 2005, pp. 61-80.
13. Jones, D. P., "Web Sag and the Effects of Camber on Steering," Proceedings of the 9th International Conference on Web Handling, ed. Good, J. K., 2007, pp. 353-370.

Name & Affiliation	**Question**
Jerry Brown, Essex Systems	How did you calculate the curvature of web?
Name & Affiliation	**Answer**
Ron Swanson, 3M Company	The curvature was calculated using equation 25 [4]. If you know the deformation of the web then the curvature can be calculated.
Name & Affiliation	**Question**
Jerry Brown, Essex Systems	Regarding Benson's work you discussed the assumption of the web sticking the roller at the first contact. You said you had reason to believe that's not true. Why's that?
Name & Affiliation	**Answer**
Ron Swanson, 3M Company	It is exactly the opposite of what we saw.
Name & Affiliation	**Question**
Jerry Brown, Essex Systems	What was it you saw that made you think that?
Name & Affiliation	**Answer**
Ron Swanson, 3M Company	We saw under high traction conditions, the web would move laterally. Benson claimed that under high traction conditions, the web would not move laterally.
Name & Affiliation	**Question**
Jerry Brown, Essex Systems	Why does that make you conclude that the web doesn't stick to the roller at first contact?
Name & Affiliation	**Answer**
Ron Swanson, 3M Company	My experimental results make me assume his model is not correct. Since most models of web lateral behavior are based on beam theory I must assume his boundary condition is not correct. I am not presenting any frictional data here.
Name & Affiliation	**Question**
John Shelton, Oklahoma State University	The assumption of perpendicularity at the entry point, especially when you deal with a laterally moving web, has concerned me from the time I was writing my dissertation. I explained this then with a sketch of a web that is slipping over a short distance dynamically as it enters a roller. For an initially straight web, the slippage is slightly modifying the length of the entering span, which is negligible. Why should a cambered web approach the line of entering contact in a perpendicular path? What law says that it will enter perpendicular? There is no law. My latest work is questioning the assumption of perpendicularity at the entry to the entering span. In other words, you have this contact patch as a separate span. It is a short span, but you have to analyze the contact patch to come up with the true boundary condition.

Name & Affiliation	Answer
Ron Swanson, 3M Company	My response to that is that everyone usually agrees that normal entry is valid. If the web enters a roller normally, you naturally think it left normally. It isn't a boundary condition that anyone has ever really questioned. The shear forces here are really quite small, not enough to account for that kind of motion, I think.